J. Membrane Biol. 183, 103–114 (2001)
DOI: 10.1007/s00232-001-0058-5

The Journal of
Membrane
Biology

Implication of the C-Terminal Region of the α-Subunit of Voltage-gated Sodium Channels in Fast Inactivation

I. Deschênes, E. Trottier, M. Chahine
Laval University, Department of Medicine, Sainte-Foy, Québec, Canada, G1K 7P4

Received: 1 March 2001/Revised: 18 May 2001

Abstract. The α-subunit of both the human heart (hH1) and human skeletal muscle (hSkM1) sodium channels were expressed in a mammalian expression system. The channels displayed slow (hH1) and fast (hSkM1) current decay kinetics similar to those seen in native tissues. Hence, the aim of this study was to identify the region on the α-subunit involved in the differences of these current-decay kinetics. A series of hH1/hSkM1 chimeric sodium channels were constructed with the focus on the C-terminal region. Sodium currents of chimeric channels were recorded using the patch-clamp technique in whole-cell configuration. Chimeras where the C-terminal region had been exchanged between hH1 and hSkM1 revealed that this region contains the elements that cause differences in current decay kinetics between these sodium channel isoforms. Other biophysical characteristics (steady-state activation and inactivation and recovery from inactivation) were similar to the phenotype of the parent channel. This indicates that the C-terminus is exclusively implicated in the differences of current decay kinetics. Several other chimeras were constructed to identify a specific region of the C-terminus causing this difference. Our results showed that the first 100-amino-acid stretch of the C-terminal region contains constituents that could cause the differences in current decay between the heart and skeletal muscle sodium channels.

This study has uncovered a direct relationship between the C-terminal region and the current-decay of sodium channels. These findings support the premise that a novel regulatory component exists for fast inactivation of voltage-gated sodium channels.

Correspondence to: M. Chahine
Mohamed.Chahine@phc.ulaval.ca

Key words: Sodium channel — Fast inactivation — Human skeletal muscle — Human heart — Electrophysiology

Introduction

Transmission of excitability throughout cells is made possible by the activation of different ion channels. Voltage-gated sodium channels play an essential role in the propagation of the action potential and cell excitability (Hodgkin & Huxley, 1952). It is the opening of these channels that is responsible for the upstroke of the action potential in excitable cells. Sodium channels are composed of an α-subunit (1800–2000 amino acids) and of smaller β-subunits (220 amino acids) (Catterall, 1992). When expressed alone in heterologous systems, the α-subunit exhibits functionality similar to the native channel demonstrating that the essential elements for sodium-channel activity are located in this subunit. Each α-subunit is comprised of four repeat transmembrane domains (D1–D4) of 250 to 300 amino acids each. Each domain is in turn composed of 6 transmembrane segments (S1–S6), with the charged S4 segment recognized as the voltage-sensor (Auld et al., 1990; Yang & Horn, 1995; Yang, George & Horn, 1996; Cha et al., 1999). It is suggested that the central ion-conducting pore is formed when the four transmembrane domains fold together, with a probable folding-back of the extracellular S5-S6 loop into the membrane, to form part of the selective permeation pathway (Backx et al., 1992; Pérez-García et al., 1996; Tsushima, Li & Backx, 1997).

Structure-function studies have also demonstrated that the region linking domains III and IV (ID III-IV) form the inactivation gate of the channel (Vassilev, Scheuer & Catterall, 1988; Patton et al., 1992; West et al., 1992; Eaholtz, Scheuer & Catterall, 1994). It is known that the ID III–IV resembles a hinged lid that

occludes the pore of the channel from the cytoplasm. A cluster of three hydrophobic amino acids (Isoleucine-Phenylalanine-Methionine, IFM) (West et al., 1992) is thought to bind to a receptor region on the cytoplasmic surface of the channel protein similar to the ball-and-chain model of the potassium channels (Armstrong & Bezanilla, 1977; Hoshi, Zagotta & Aldrich, 1990). The S4-S5 linkers of domains III and IV may form the proposed receptor site (Tang et al., 1996; Smith & Goldin, 1997; Filatov et al., 1998; McPhee et al., 1998). The mechanism by which the inactivation particle (IFM) binds to the proposed receptor produces fast inactivation. Sodium channels also undergo a slow mode of inactivation. The regions of the channel implicated in slow inactivation are not well characterized. However, mutations in the pore regions of the different domains have been observed to affect slow inactivation (Bénitah et al., 1999; Todt et al., 1999; Townsend & Horn, 1999). This suggests that the pore region is associated with this mechanism.

However, little is known about the function of the C-terminal region in voltage-gated sodium channels. Recent mutations on the C-terminal region of the human heart sodium channel were observed to disrupt fast inactivation in patients suffering from the long-QT syndrome (Wei et al., 1999; Deschênes et al., 2000).

Sodium channels cloned from the human heart (hH1) (Gellens et al., 1992) and human skeletal muscle (hSkM1) (George, Jr. et al., 1992) show slow and fast current decay, respectively, when expressed in a mammalian cell line as it is seen in native tissues (Chahine et al., 1993; Chahine et al., 1996; Wang, George, Jr. & Bennett, 1996). We have previously shown that the domain IV or the C-terminal region of the α-subunit, or both, are responsible for the differences seen in current decay between the human heart and the rat skeletal muscle isoforms (Deschênes et al., 1998). The aim of this study was to localize the area of the C-terminus of the α-subunit responsible for the distinct current decay kinetics seen between the human heart and human skeletal muscle sodium channels.

Materials and Methods

Recombinant DNA Constructions of Chimeric Channels

For the chimeras constructed with the parent channel of hH1, restriction enzyme sites were introduced by site-directed mutagenesis as silent mutations on a *Sac*II (4466)-*EcoR*1 (6146) hSkM1/C-terminal fragment of about 1800 base pair (bp) cloned in pBluescript. A *Xba*1 site was introduced at position 4868 of this hSkM1/C-terminal fragment. An *Eag*1 (5279)-*Spe*1 (7591) hH1/C-terminal fragment of about 2300 bp was also cloned in pBluescript and a *Xba*1 site was also introduced at position 5463. Fragment *Xba*1-*EcoR*1 of hSkM1 was ligated to fragment *Eag*1-*Xba*1 of hH1 which gives the pre-HS, and fragment *Xba*1-*EcoR*1 of hH1 was ligated to fragment *Sac*II-*Xba*1 of hSkM1, which gives pre-SH. The same protocol was used to introduce *Bss*HII (position 5877 on hH1, 5282 on hSkM1) and *Dra*I (position 5762 on hH1, 5167 on hSkM1) sites via silent mutations.

pCDNA1/HS consists of pcDNA1 (4.8 kb with *Hind*III and *Xho*1 ends), with fragment *Hind*III-*Eag*1 of hH1 (5279 bp), and fragment pre-HS (1500 bp) which consists of hH1/*Eag*1-*Xba*1 (184 bp) and hSkM1/*Xba*1-*Xho*1 (~1300 bp) (Fig. 4*A*).

pcDNA1/SH consists of pcDNA1/hSkM1 (without a fragment *Cla*1-*Xba*1 of 1531 bp), ligated to fragment pre-SH that consists of hSkM1/*Cla*1(4615)-*Xba*1(4868) (253 bp) and hH1/*Xba*1-*Spe*1 (~2100 bp). (*Spe*1 and *Xba*1 have cohesive ends) (*see* Fig. 4*A*).

pCDNA1/HHS consists of pcDNA1 (4.8 kb with *Hind*III and *Xho*1 ends), with fragment *Hind*III-*Eag*1 of hH1 (5279 bp), and a fragment (~1500 bp) which consists of hH1/*Eag*1-*Xba*1 (184 bp), hH1/*Xba*1-*Bss*HII (414 bp) and hSkM1/*Bss*HII-*Xho*1 (~1000 bp) (*see* Fig. 4*A*).

pcDNA1/SSH consists of pcDNA1/hSkM1 (without a fragment *Cla*1-*Xba*1 of 1531 bp), ligated to a fragment that consists of hSkM1/*Cla*1(4615)-*Xba*1(4868) (253 bp), hSkM1/*Xba*1-*Bss*HII (414 bp) and hH1/*Bss*HII-*Spe*1 (1713 bp). (*Spe*1 and *Xba*1 have cohesive ends) (*see* Fig. 4*A*).

pcDNA1/SS^{100AA}H consists of pcDNA1/hSkM1 (without a fragment *Cla*1-*Xba*1 of 1531 bp), ligated to a fragment that consists of hSkM1/*Cla*1(4615)-*Xba*1(4868) (253 bp), hSkM1/*Xba*1-*Dra*1 (299 bp) and hH1/*Dra*1-*Spe*1 (1828 bp). (*Spe*1 and *Xba*1 have cohesive ends) (*see* Fig. 4*A*).

Chimeric channel, mutants, wild-type hH1 and hSkM1 in pcDNA1 construct were purified using Qiagen columns (Qiagen, Chatsworth, CA, USA).

Mutagenesis

The QuickChange™ site-directed mutagenesis kit from Stratagene (La Jolla, CA, USA) was used according to the manufacturer's instructions to create silent mutants for the generation of chimeric channels and the following C-terminus mutations: S1776N, T1783S, D1792E, I1797T, E1804D, E1810A, V1813R, A1818V, A1820T, S1822Q, Q1832K, S1834K, N1837T, M1838L, S1844P, R1847K, M1851L, F1857L, R1860E, E1864D (*see* Fig. 4*B*). All mutations were confirmed by sequencing.

Transfections of the tsA201 Cell Line

The tsA201 cell line is a mammalian cell line derived from human embryonic kidney HEK 293 cells by stable transfection with SV40 large T antigen. Cells were grown in high glucose DMEM supplemented with FBS (10%), L-glutamine (2 mM), penicillin (100 U/ml) and streptomycin (10 mg/ml) (Gibco BRL Life Technologies, Burlington, Ontario, Canada). Cells were incubated in a 5% CO_2 humidified atmosphere. Transfections of tsA201 cells were carried out using the calcium phosphate method (Margolskee, McHendry-Rinde & Horn, 1993) with the following modification to facilitate the identification of individual transfected cells: a cotransfection with an expression plasmid for a lymphocyte surface antigen was made (CD8-a) (Jurman et al., 1994). 10 μg of cDNAs encoding for wild-type (hH1 and hSkM1), chimeras or mutant sodium channels with 10 μg of CD8-a were used. For patch-clamp experiments, cells were used 2 to 3 days posttransfection. The cells were incubated in a medium containing anti-CD8-a-coated beads for 2 minutes (Dynabeads M-450 CD8-a) and the unattached beads were washed away. Beads were prepared according to the manufacturer's instructions (Dynal A.S., Oslo, Norway). Cells ex-

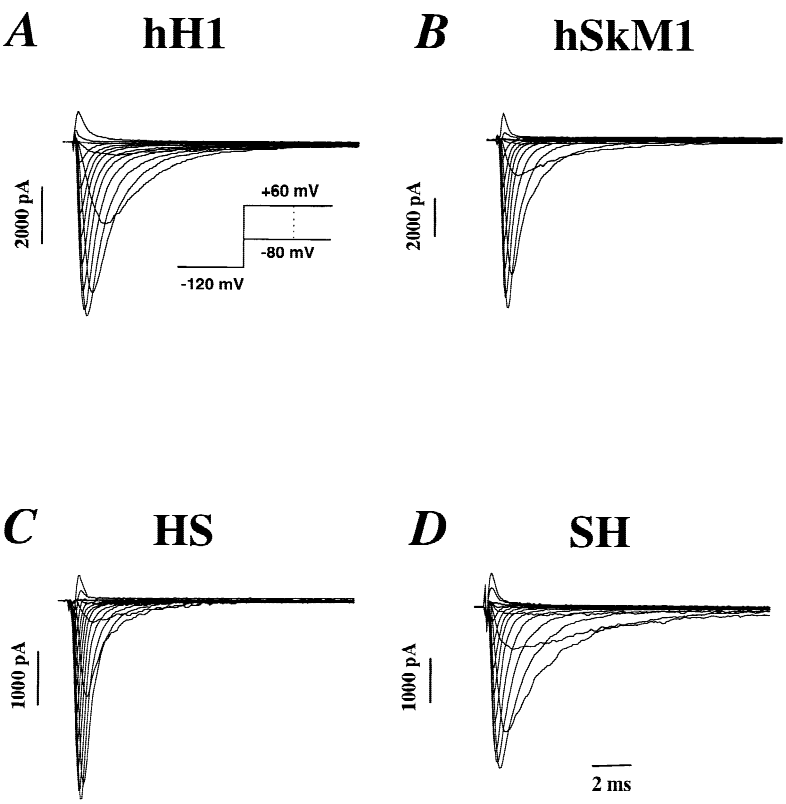

Fig. 1. Family of inward and outward sodium currents. Currents were recorded from a holding potential of −120 mV from −80 mV to +60 mV in 10 mV steps of 15 msec duration, for wild-type hH1 (*A*), wild-type hSkM1 (*B*) and chimeras formed from these isoforms (HS and SH, H: heart, S: skeletal muscle). Note that the C-terminal region was exchanged between hH1 and hSkM1 to form HS (*C*), and SH (*D*). HS has the C-terminal region of hSkM1 and SH has the C-terminal region of hH1.

pressing surface CD8-a fixed the beads and were visually distinguishable under the microscope from nontransfected cells.

Patch Clamp Methods

Macroscopic sodium currents from transfected cells were recorded using the whole-cell patch-clamp technique (Hamill et al., 1981). Patch electrodes were made from 8161 Corning glass and coated with Sylgard (Dow-Corning, Midland, MI, USA) to minimize their capacitance. Low resistance electrodes (<2MΩ) were used, and a routine series-resistance compensation of an Axopatch 200 amplifier was performed to values >80% to minimize voltage-clamp errors. To ensure the quality of the voltage clamp, we measured the time constant of membrane charge capacitance ($\tau = R_{series} \cdot C_m$) $\tau = 4.71 \pm 0.43$ μs, $n = 40$. The C_m and R_{series} were obtained, respectively, from the capacitance and the series resistance compensation of the Axopatch 200. Voltage-clamp command pulses were generated by microcomputer using pCLAMP software v5.5 (Axon Instruments, Foster City, CA, USA). Recorded membrane currents were filtered at 5 kHz. Experiments were performed 10 minutes after entering whole-cell configuration to allow current to stabilize. To minimize the influence of time-dependent shifts in gating, recordings for hH1, hSkM1 and all the chimeras were systematically made in the same order: *I/V* curve, steady-state inactivation, recovery from inactivation (HP = −120 mV), ten minutes after breaking the seal.

Solutions and Reagents

For whole-cell recordings, the patch pipette contained (in mM): 35 NaCl; 105 CsF; 10 EGTA; and 10 Cs-HEPES (pH = 7.4). The bath solution contained (in mM): 150 NaCl; 2 KCl; 1.5 $CaCl_2$; 1 $MgCl_2$; 10 glucose; and 10 Na-HEPES (pH = 7.4). A correction of the liquid junction potential of −7 mV between patch pipette and bath solutions was made. Experiments were performed at room temperature (22–23°C).

Statistical Analysis

Data are expressed as mean ± SEM. When indicated, *t*-test analysis was assessed using statistical software in SigmaPlot (Jandel Scientific Software, San Rafael, CA, USA). Differences were deemed significant at a P value <0.05.

Results

Chimeras HS and SH

Current Decay Kinetics

Families of sodium currents from tsA201 cells transfected with the parent channels (hH1 and hSkM1) were recorded (Fig. 1*A* and *B*). The figure shows that the decays after peaking of the sodium current of hH1 and hSkM1 are different, hH1 current decays being slower. To study the rate of inactivation, sodium currents were recorded from a holding potential of −120 mV starting at −80 mV to +60 mV in 10 mV increments for 15 msec

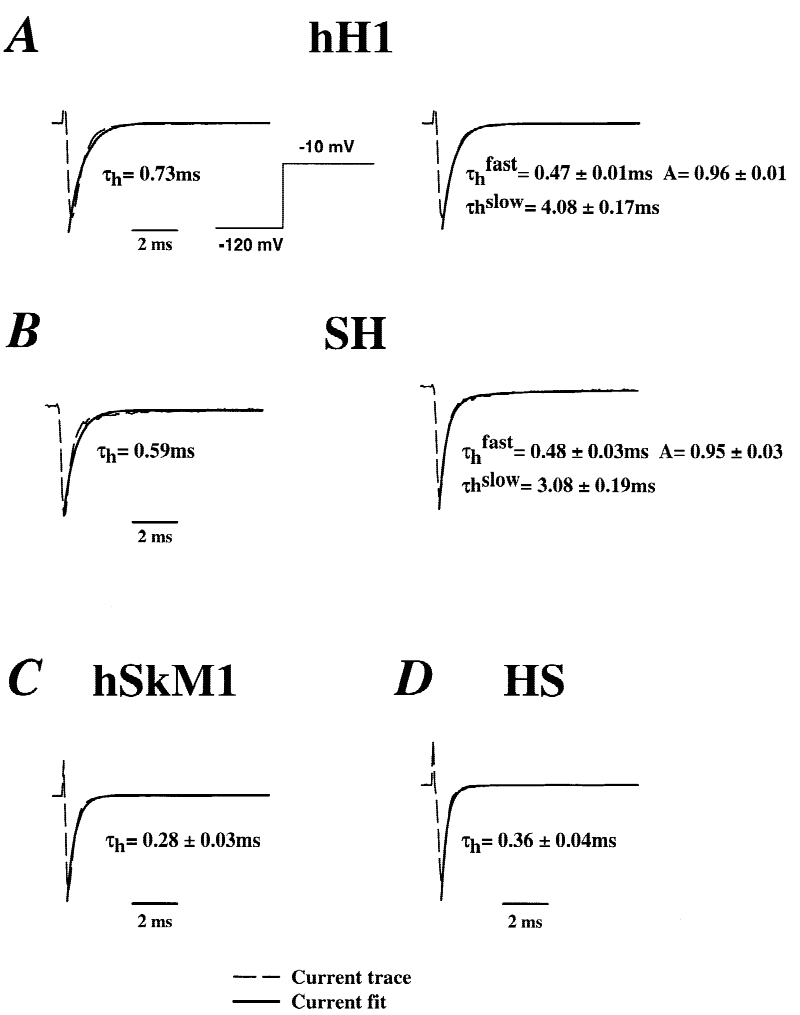

Fig. 2. Whole-cell inward sodium currents. Currents were recorded at −10 mV test pulse from a −120 mV holding potential for: hH1 (*A*), SH (*B*), hSkM1 (*C*) and HS (*D*), HS and SH being the chimeric channels created from hSkM1 and hH1. Currents from hH1 and SH were fitted with a single-time constant exponential function (*left*) (τ_h represent the time constant of the exponential fit) or with a two-time-constants exponential function (*right*) where the time constants values and amplitude associated with fast (τ_h^{fast}) and slow (τ_h^{slow}) were indicated. Currents from hSkM1 and HS were fitted with only one time constant (τ_h).

(Current/Voltage or *I/V* protocol) (Fig. 1*A* and *B*). The best fit for current decay was done using a single-exponential function for hSkM1 (τ_h) and two exponentials for hH1 (τ_h^{fast} and τ_h^{slow}; Fig. 2). The amplitude of the slow *vs.* fast components shows some variability from cell to cell, however, it does not appear to be voltage dependent. Thus, it seems that the different current-decay behaviors of the skeletal and cardiac sodium channels are strictly related to the presence of a slow component of inactivation for hH1 and not to its amplitude. This was true for both inward and also outward sodium currents measured at +60 mV where inactivation is not influenced by activation (Fig. 2*A* and 2*C*, Fig. 3*A* and *C* and Table 1).

In a previous study (Deschênes et al., 1998), we showed that the structural basis for the differences in current decay seen between hH1 and rSkM1 were either located in domain IV and/or in the C-terminus of the α-subunit of voltage-gated sodium channels. Although the rat and the human skeletal muscle isoforms have similar biophysical behavior, in this study we used the human heart (hH1) and human skeletal muscle (hSkM1) sodium channel isoforms to obtain same-species chimeras. We created hH1/hSkM1 chimeric sodium channels by first exchanging the C-terminal region between hH1 and hSkM1 (Fig. 4*A*). The first chimera HS contained the parent channel hH1 (N-terminus-DI to DIV) with the C-terminal region of hSkM1. A typical family of sodium currents recorded with the *I/V* protocol from transfected cells expressing HS showed fast current decay (Fig. 1*C*) and the inactivation kinetics were best fitted with one time constant (τ_h) as was the case for hSkM1 sodium currents (Fig. 2*D*, for inward currents; Fig. 3*D* for outward currents and Table 1). Since HS exhibited current-decay kinetics similar to those of hSkM1, we were able to conclude that the C-terminal region caused the differences observed between the two isoforms for this biophysical parameter. To confirm our results, we constructed the reverse chimera SH, which corresponded to the parent channel of hSkM1 and the C-terminal region of hH1 (Fig. 4*A*). Currents from this chimera were also recorded using the *I/V* protocol (Fig. 1*D*) and currents

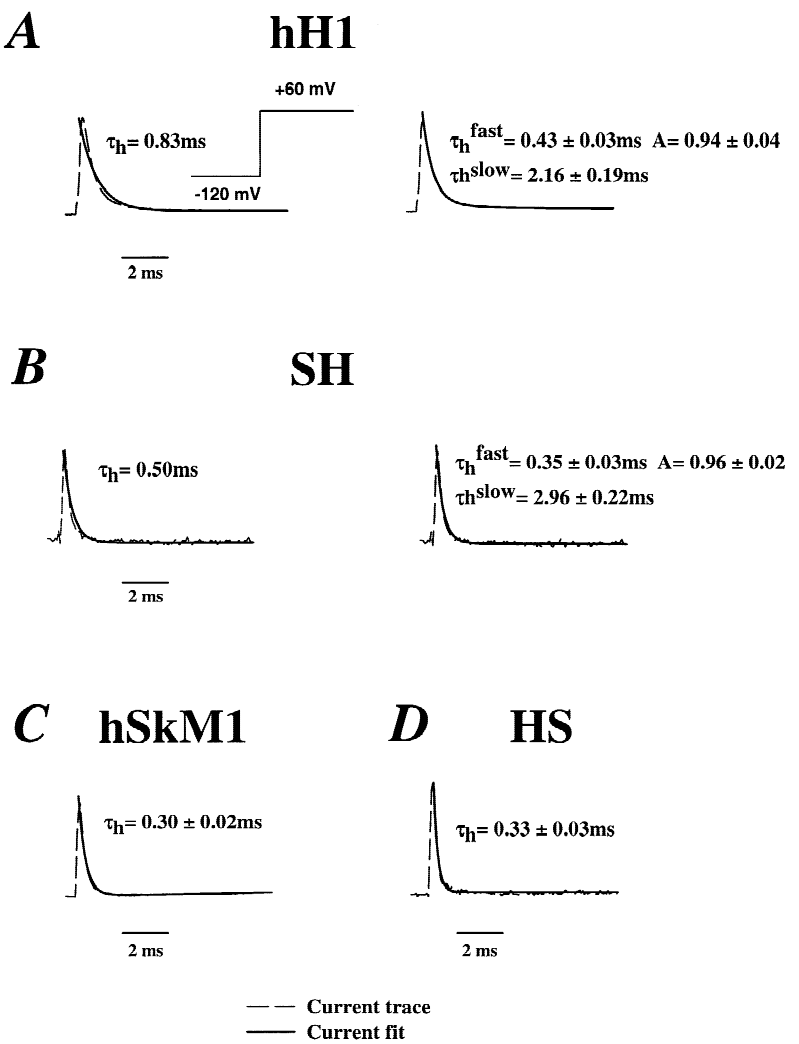

Fig. 3. Whole-cell outward sodium currents. Currents were recorded at +60 mV test pulse from a −120 mV holding potential for: hH1 (*A*), SH (*B*), hSkM1 (*C*) and HS (*D*), HS and SH being the chimeric channels created from hSkM1 and hH1. Currents from hH1 and SH were fitted with a single-time-constant exponential function (*left*) (τ_h represents the time constant of the exponential fit) or with a two-time-constants exponential function (*right*), where the time constant values and amplitude associated with fast (τ_h^{fast}) and slow (τ_h^{slow}) were indicated. Currents from hSkM1 and HS were fitted with only one time constant (τ_h).

decayed with two time constants as for hH1 (τ_h^{fast} and τ_h^{slow}) (Fig. 2*B*, for inward currents; Fig. 3*B*, for outward currents and Table 1). The voltage dependence of time constants of all the chimeras used in this study was plotted in Fig. 5*A*. These data confirm the role of the C-terminal region in the fast inactivation of voltage-gated sodium channels.

Steady-state Activation and Inactivation

Steady-state activation curves (G_v curves) were constructed from *I/V* plots and fitted with a Boltzmann function. While G_v curves of hH1 and hSkM1 were shifted by 20 mV, G_v of HS and SH chimeras behaved as the parental channels (Fig. 5*B*).

Steady-state inactivation was studied by a two-pulse protocol with 500 msec depolarizing prepulses from a holding potential of −140 mV stepped from −140 to −30 mV in 10 mV increments followed by a −30 mV test pulse. Each experiment was fitted with a Boltzmann equation, which provides the voltage at which 50% of the channels is inactivated ($V_{1/2}$), and the slope factor (k_v) parameters for each channel studied (Fig. 5*B* and Table 1). The heart isoform inactivated at more negative voltages than the skeletal muscle isoform (hH1: $V_{1/2} = -100 \pm 1.4$ mV, $k_v = 5.7 \pm 0.2$; hSkM1: $V_{1/2} = -88.2 \pm 2.1$ mV, $k_v = 6.0 \pm 0.2$) (Fig. 5*B* and Table 1). The results with the chimeric channels HS and SH showed that the steady-state inactivation parameters are comparable to the ones of the parental channels (Fig. 5*B* and Table 1). This indicates that the C-terminal region is not structurally implicated either in steady-state activation or in steady-state inactivation parameters differences.

Recovery from Inactivation

The recovery from inactivation was studied with a two-pulse protocol at two holding potentials, −120 mV and −100 mV (Fig. 5*C*, shown for −120 mV, and Table 1). A prepulse of 40 msec depolarization to −20 mV was

Table 1. Inactivation and recovery from inactivation parameters of parent channels and chimeras.

Channel type	Steady-state activation (mV)	Steady-state inactivation (mV)	Recovery from inactivation τ_{rec} (msec)		Time constant of inactivation τ_h (msec) (−10 mV)	*n*
			HP = −120 mV	HP = −100 mV		
hH1	$V_{1/2} = -53.6 \pm 2.0^a$ $k_v = 6.4 \pm 0.9$	$V_{1/2} = -100.0 \pm 1.4^c$ $k_v = 5.7 \pm 0.2$	12.7 ± 0.4^e	51.9 ± 5.8^g	$\tau_h^{fast} = 0.53$ $\tau_h^{slow} = 4.8 \pm 0.1$	6
hSkM1	$V_{1/2} = -32.2 \pm 2.6^b$ $k_v = 8.2 \pm 0.6$	$V_{1/2} = -77.6 \pm 2.7^d$ $k_v = 6.5 \pm 0.4$	6.2 ± 0.3^f	12.2 ± 1.1^h	$\tau_h = 0.44 \pm 0.12$	6
HS	$V_{1/2} = -52.8 \pm 1.4^a$ $k_v = 6.9 \pm 0.5$	$V_{1/2} = -98.8 \pm 3.9^c$ $k_v = 5.7 \pm 0.7$	11.4 ± 0.2^e	47.3 ± 4.8^g	$\tau_h = 0.53 \pm 0.02$	5
SH	$V_{1/2} = -35.6 \pm 2.3^b$ $k_v = 7.5 \pm 0.3$	$V_{1/2} = -71.1 \pm 1.7^d$ $k_v = 5.3 \pm 0.2$	5.4 ± 0.2^f	8.5 ± 1.8^h	$\tau_h^{fast} = 0.48 \pm 0.03$ $\tau_h^{slow} = 3.08 \pm 0.19$	4
HHS		$V_{1/2} = -101.1 \pm 3.1^c$ $k_v = 5.4 \pm 0.4$	15.9 ± 2.0^e		$\tau_h^{fast} = 0.68 \pm 0.03$ $\tau_h^{slow} = 3.82 \pm 0.14$	4
SSH		$V_{1/2} = -81.0 \pm 3.2^d$ $k_v = 5.4 \pm 0.3$	6.4 ± 1.2^f		$\tau_h = 0.54 \pm 0.04$	5
$SS^{100aa}H$		$V_{1/2} = -79.2 \pm 2.1^d$ $k_v = 5.2 \pm 1.0$	5.3 ± 0.4^f		$\tau_h = 0.53 \pm 0.05$	5

$V_{1/2}$: midpoint of steady-state activation and inactivation; k_v: slope factor of steady-state activation and inactivation; HP: holding potential; *n*: Number of cells tested.
Superscripts a–h indicate that there was no statistically significant difference ($P > 0.05$) between the values bearing identical superscripts.

followed at various time intervals with a 40 msec test pulse to −20 mV. The amplitude of the test pulse currents was normalized with the amplitude of the prepulse currents and the results were fitted with a single exponential function, with a recovery time constant τ_{rec}. For example at a holding potential of −120 mV, hSkM1 has a τ_{rec} value of 6.2 ± 0.3 msec while hH1 recovers slower with a τ_{rec} value of 12.7 ± 0.4 msec. The time constants of recovery from inactivation of HS and SH chimeras were not significantly different from the one of the parental channels (Fig. 5*C*, shown for −120 mV, and Table 1). These data indicate that the C-terminal region is not implicated in differences between hH1 and hSkM1 in this biophysical mechanism.

Chimeras HHS, SSH and $SS^{100AA}H$

We constructed additional C-terminal chimeras to identify which amino acid(s) within the C-terminal region was/were implicated in fast inactivation and responsible for the differences seen between hH1 and hSkM1. A chimera containing the parent channel (N-terminus-DI to DIV) and the first 139 amino acids of hH1 and the last 105 C-terminal amino acids of hSkM1 was created (HHS) (Fig. 4*A*). We expressed this chimera in tsA201 cells and recorded sodium currents using the *I/V* protocol (Fig. 6*A*). The best current-decay fit of these currents was obtained using two exponential functions, as with hH1 (τ_h^{fast} and τ_h^{slow}) (Fig. 7*A*, for inward currents; Fig. 8*A* for outward currents and Table 1). These data suggested that the amino acid(s) implicated is or are located in these first 139 amino acids of the C-terminal region. We confirmed these results by expressing the reverse chimera SSH. This chimera was formed by the parent channel and the first 139 amino acids of the C-terminal region of hSkM1 and the last 105 amino acids of the C-terminus of hH1 (Fig. 4*A*). The expressed sodium currents exhibited a fast current decay (Fig. 6*B*) which was best fitted with a single exponential function resulting in one time constant (τ_h) as seen for hSkM1 (Fig. 7*B*, for inward currents; Fig. 8*B* for outward currents, and Table 1).

We constructed a last chimera, $SS^{100aa}H$ chimera, which was formed with the parent channel and the first 100 amino acids of the C-terminus of hSkM1 and the last 144 amino acids of the C-terminus of hH1 (Fig. 4*A*). The currents recorded from cells transfected with $SS^{100aa}H$ under the *I/V* protocol showed fast inactivating currents (Fig. 6*C*) that were best fitted with a single-exponential function (Fig. 7*C*, for inward currents; Fig. 8*C*, for outward currents, and Table 1). The current-decay phenotype of this chimera corresponded to hSkM1 indicating that the amino acids responsible for the differences between hH1 and hSkM1 are within these first 100 amino acids of the C-terminal region. The voltage dependence of the time constants of HHS, SSH and $SS^{100aa}H$ chimeras are reported in Fig. 5*A*.

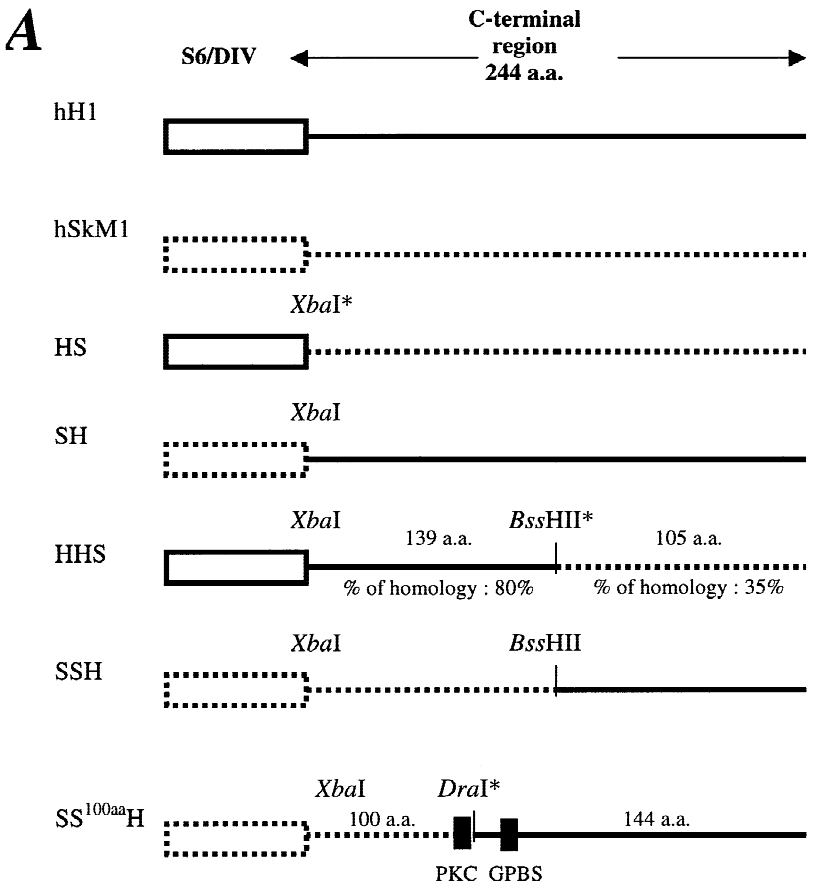

B

```
hH1       1773 ENFSVATEESTEPLSEDDFDMFYEIWEKFDPEATQFIEYSVLSDFADALSEPLRIAKPNQ 1833
               ||| |||||| ||| |||| |||| |||||| ||||| || |||| | | |||||||||
hSKM1     1609 ENFNVATEESSEPLGEDDFEMFYETWEKFDPDATQFIAYSRLSDFVDTLQEPLRIAKPNK 1669

hH1       1834 ISLINMDLPMVSGDRIHCMDILFAFTKRVLGESGEMDALKIQMEEKFMAANPSKISYEPI 1893
               | ||  ||||| || ||| ||||| || ||| |||||||| ||||||||||| |||||
hSKM1     1670 IKLITLDLPMVPGDKIHCLDILFALTKEVLGDSGEMDALKQTMEEKFMAANPSKVSYEPI 1729

hH1       1894 TTTLRRKHEEVSAMVIQRAFRRHLLQRSLKHASFLFRQQAGSGLSEEDAPEREGLIAYVM 1951
               |||| |||||| |  |||| |||||||| | ||   |       |  |||| ||| |  |
hSKM1     1730 TTTLKRKHEEVCAIKIQRAYRRHLLQRSMKQASYMYR--HSHDGSGDDAPEKEGLLANTM 1789

hH1       1952 SENFSRPLGPPSSSSISSTSFPPSYDSVTRATSDNLQVRGSDYSHSEDLADFPPSPDRDR 2002
               |       |  ||         ||      |  |     |       | |  |  |
hSKM1     1790 SKMYGHENGNSSS---------PSPEEKGEA-GDAGPTMGLMPISPSDTAWPPAPPPGQT 1850

hH1       2003  ------ESIV 2013
                      || |
hSKM1     1851  VRPGVKESLV 1855
```

Fig. 4. Chimera construction and amino-acid sequence of hH1 and hSkM1. (*A*) Schematic illustration of the chimeric channels between hH1 and hSkM1 involving the C-terminal region of the α-subunit of voltage-gated sodium channels. * denotes enzyme restriction site introduced by site-directed mutagenesis to facilitate the making of the chimeras; PKC, phosphorylation site of protein kinase C (TKR); GPBS, binding site of G protein (QMEEK). (*B*) Alignment of the C-terminal region of hH1 and hSkM1. The homology between the two isoforms is illustrated. The amino acids represented in bold are, respectively, the localization of long-QT mutation (E1784) and the phosphorylation site of the PKC (TKR).

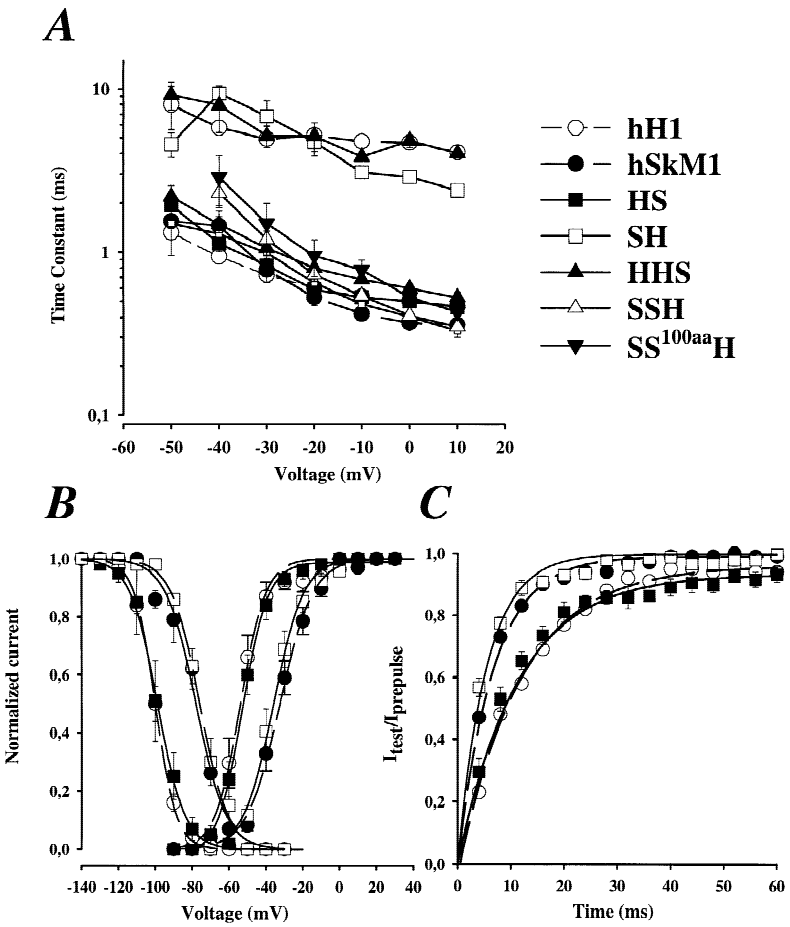

Fig. 5. Gating properties of hH1, hSkM1 and their chimeric channels. (*A*) Voltage-dependence of time constants of inactivation for hH1, hSkM1 and HS and SH chimeras. Current decays after the peak at different voltages were fitted with a single exponential (τ_h) for hSkM1, HS, SSH and $SS^{100aa}H$. For hH1, SH and HHS, the falling phase of each record needed to be fitted with two exponentials (τ_h^{fast} and τ_h^{slow}). (*B*) Voltage-dependence of steady-state activation (G_v) and inactivation (h_∞) of hH1, hSkM1, HS and SH. For steady-state inactivation a two-pulse protocol was used with 500 msec prepulse ranging from −140 mV to −30 mV. The G_v and h_∞ curves were fitted to a Boltzmann distribution $I/I_{max} = 1/1+\exp((V-V_{1/2})/k_v)$ with given $V_{1/2}$ and k_v values. (*C*) Time course of recovery from inactivation was studied using a two-pulse duration at −20 mV measured at interpulse intervals of 4 msec from a holding potential of −120 mV. The solid line shows the fit of the data using the following equation $I_{test}/I_{prepulse} = 1 - \exp(-t/\tau_{rec})$.

As seen for chimeras HS and SH, steady-state inactivation and recovery from inactivation parameters of HHS, SSH and $SS^{100aa}H$ chimeras were comparable to those of the parent channel (Table 1).

Single Mutations

Sequence comparison of the first 100-amino-acids stretch of the C-terminus show that the region differs by 20 amino acids (Fig. 4*B*). We mutated these 20 amino acids on the hH1 sodium channel by individually replacing them with their hSkM1 equivalent (*see* Materials and Methods for the enumeration of mutants). Sodium currents were recorded from tsA201 cells using the same *I/V* protocol at a holding potential of −120 mV (as was used to screen the chimeras). All the mutants showed current-decay kinetics that corresponded to hH1 with two time constants of current decay (τ_h^{fast} and τ_h^{slow}) (Table 2). This indicates that a combination of these residues is most likely involved in the differences in current decay. For steady-state inactivation and recovery from inactivation parameters, again the data were comparable to those of the parent channel (*data not shown*).

Discussion

In native tissues, voltage-gated sodium channels from the heart and skeletal muscle have different pharmacological and biophysical properties (Frelin et al., 1986; Kirsch & Brown, 1989; Ravindran, Schild & Moczydlowski, 1991; Schild & Moczydlowski, 1991; Arreola, Spires & Begenisich, 1993). When the cloned α-subunit cDNAs from the heart and skeletal muscle sodium channels were expressed in a mammalian cell line, they had biophysical characteristics similar to those seen in native tissues (Chahine et al., 1993; Chahine et al., 1996; Wang et al., 1996). The studied parameters that differ between the two isoforms are steady-state activation, current-decay kinetics, steady-state inactivation, and recovery from inactivation. This suggests that the α-subunit of voltage-gated sodium channels contains the structural basis for these biophysical parameters. In a previous study, we examined the correlation of each of those parameters to a restricted portion of the α-subunit. Chimeric channels between the human heart isoform (hH1) (Gellens et al., 1992) and rat skeletal muscle isoform (rSkM1) (Trimmer et al., 1989) were constructed (Deschênes et al., 1998). It was established that the DIV and/or the C-terminal

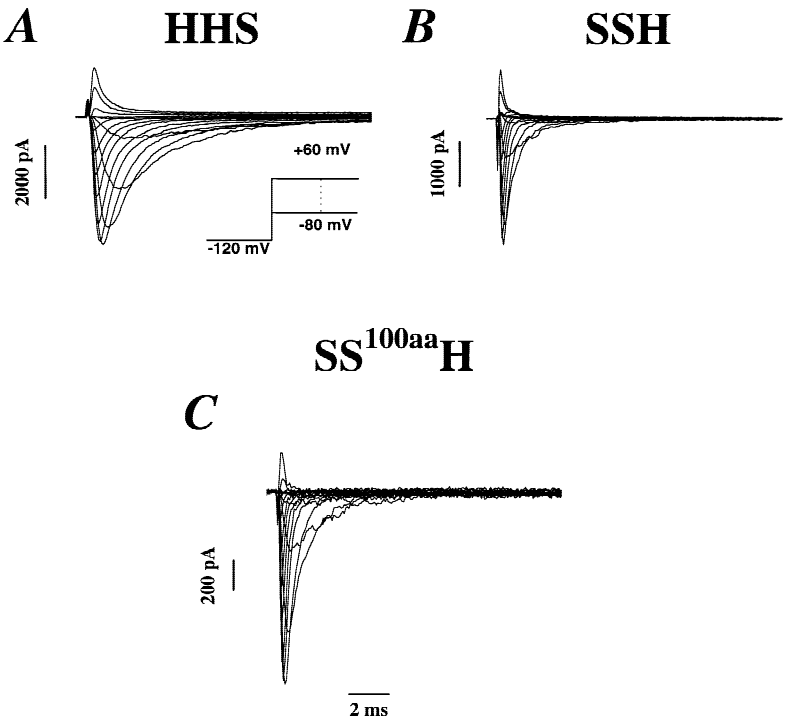

Fig. 6. Family of inward and outward sodium currents recorded from cells expressing HHS (*A*), SSH (*B*) and SS^{100aa}H (*C*) chimeras (*see* Fig. 4 for details). Currents were generated from a holding potential of −120 mV to +60 mV in 10 mV steps of 15 msec duration.

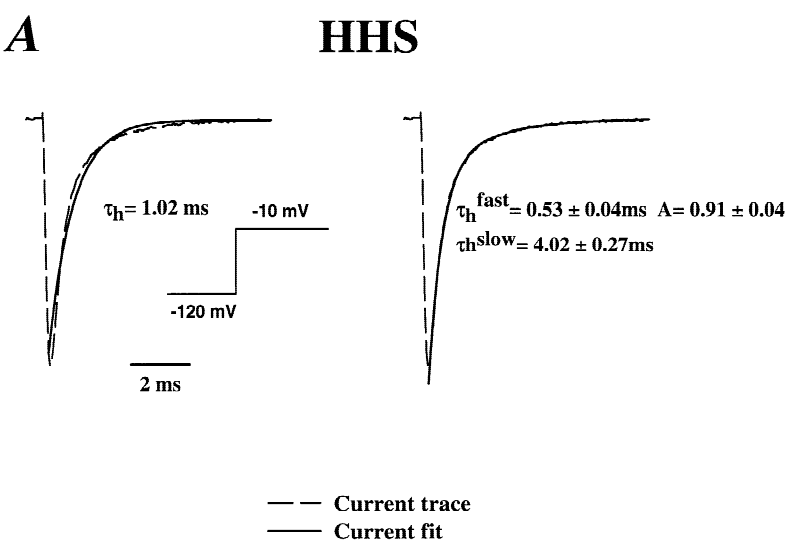

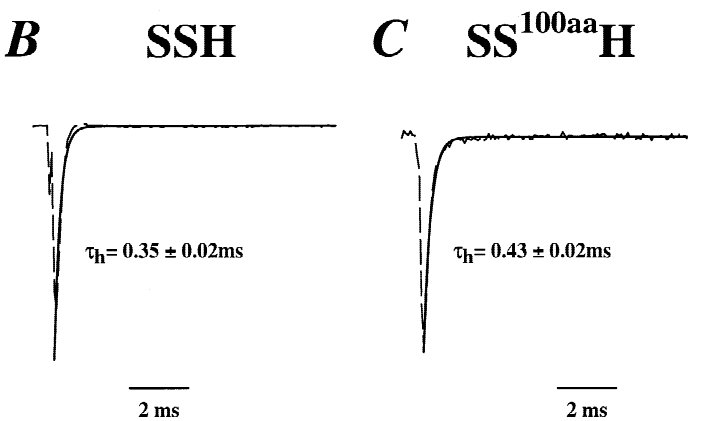

Fig. 7. Whole-cell inward sodium currents elicited by a test pulse of −10 mV from a holding potential of −120 mV of HHS (*A*), SSH (*B*) and SS^{100aa}H (*C*). (*A*) Currents were fitted with a single-time-constant exponential function (*left*) (τ_h represents the time constant of the exponential fit) or with a two-time-constants exponential function (*right*) where the time constant values and amplitude associated with fast (τ_h^{fast}) and slow (τ_h^{slow}) were indicated. (*B*) and (*C*) Currents required only a single-exponential function to be fitted.

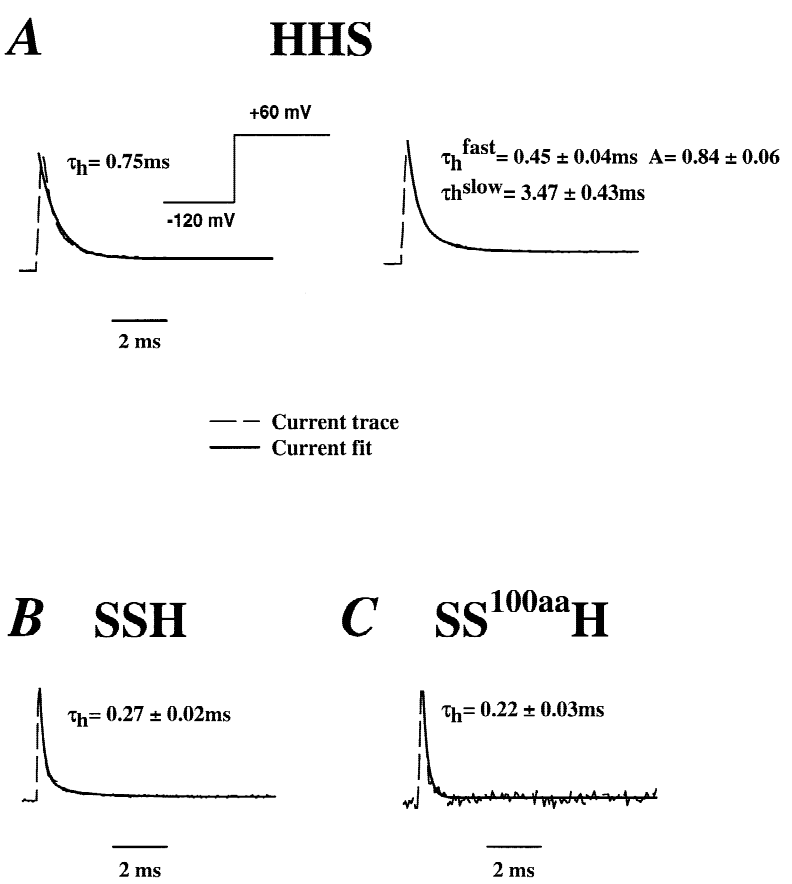

Fig. 8. Whole-cell outward sodium currents elicited by a test pulse of +50 mV from a holding potential of −120 mV of HHS (*A*), SSH (*B*) and $SS^{100aa}H$ (*C*). (*A*) Currents were fitted with a single-time-constant exponential function (*left*) (τ_h represents the time constant of the exponential fit) or with a two-time-constants exponential function (*right*) where the time constant values and the amplitude associated with fast (τ_h^{fast}) and slow (τ_h^{slow}) are indicated. (*B*) and (*C*) Currents required only a single exponential function to be fitted.

region of the α-subunit were responsible for the differences in current decay kinetics between heart and skeletal muscle channels. The other biophysical differences between hH1 and rSkM1, such as steady-state activation and inactivation and recovery from inactivation, are probably determined by more than one domain of the α-subunit.

The objective of this study was to localize the specific regions of the DIV and/or the C-terminus implicated in current decay kinetics seen between the human heart (hH1) and human skeletal muscle (hSkM1) sodium channel isoforms. Since the τ_h of hSkM1 was comparable to τ_h^{fast} of hH1, this suggested that differences in current decay reside in the presence or not of a slow component, this holds true for all the chimeras studied. Chimeric channels where the C-terminal region was exchanged were constructed and expressed in tsA201 cells. Steady-state inactivation and recovery from inactivation parameters of the chimeras were consistent with those of the parent channels (Table 1). These data indicated that the portion of the α-subunit implicated in these mechanisms is located in N-terminus DI to DIV. However, the chimera constructed with the C-terminal region of hSkM1 (HS) had current-decay kinetics that corresponded to the skeletal muscle phenotype. Conversely, chimera SH which had the C-terminus of hH1 showed slower current-decay kinetics as was seen for the heart channel, with two time constants of current decay (Table 1). This indicates that the C-terminal region probably possesses the structure implicated in current-decay kinetics that confers the different phenotype to the two isoforms.

The use of other chimeras allowed us to narrow the region implicated in hH1 and hSkM1 kinetics down to 100 amino acids of the C-terminus. It was previously shown that G proteins binding to the C-terminal region affects inactivation of the brain sodium channels (Ma, Catterall & Scheuer, 1997). However, the conserved G protein binding site (QMEEK) of hH1 and hSkM1 is not included in this same 100-amino-acid stretch (Fig. 4*B*). Thus, the G proteins would not be responsible for the difference seen in current-decay kinetics between the heart and the skeletal muscle. Single reverse mutations of the 20 amino acids in this 100-amino-acid stretch were unsuccessful in assigning the differences in current decay between hH1 and hSkM1 to just one amino acid (Table 2). Furthermore, the single reverse mutation (R1860E) at the PKC phosphorylation site of hH1 (TKR) (Fig. 4*B*), is not responsible for differences in current-decay phenotypes between the two isoforms.

Table 2. Time constants of current decay for the single mutations

Channel	Time constant of inactivation τ_h (msec) (−10 mV)	*n*	Channel	Time constant of inactivation τ_h (msec) (−10 mV)	*n*
hH1	$\tau_h^{fast} = 0.53$ $\tau_h^{slow} = 4.8 \pm 0.1$	6	hH1/S1822Q	$\tau_h^{fast} = 0.48 \pm 0.03$ $\tau_h^{slow} = 4.14 \pm 0.41$	5
hSkM1	$\tau_h = 0.44 \pm 0.12$	6	hH1/Q1832K	$\tau_h^{fast} = 0.52 \pm 0.01$ $\tau_h^{slow} = 5.51 \pm 0.90$	3
hH1/S1776N	$\tau_h^{fast} = 0.59 \pm 0.05$ $\tau_h^{slow} = 3.41 \pm 0.1$	3	hH1/S1834K	$\tau_h^{fast} = 0.51 \pm 0.01$ $\tau_h^{slow} = 4.72 \pm 0.70$	4
hH1/T1783S	$\tau_h^{fast} = 0.41 \pm 0.02$ $\tau_h^{slow} = 5.96 \pm 1.01$	4	hH1/N1837T	$\tau_h^{fast} = 0.48 \pm 0.01$ $\tau_h^{slow} = 4.55 \pm 0.19$	6
hH1/D1792E	$\tau_h^{fast} = 0.55 \pm 0.08$ $\tau_h^{slow} = 4.57 \pm 0.39$	4	hH1/M1838L	$\tau_h^{fast} = 0.54 \pm 0.02$ $\tau_h^{slow} = 4.61 \pm 0.15$	3
hH1/I1797T	$\tau_h^{fast} = 0.49 \pm 0.10$ $\tau_h^{sow} = 4.52 \pm 0.35$	5	hH1/S1844P	$\tau_h^{fast} = 0.57 \pm 0.07$ $\tau_h^{slow} = 5.91 \pm 0.82$	3
hH1/E1804D	$\tau_h^{fast} = 0.45 \pm 0.06$ $\tau_h^{slow} = 4.82 \pm 0.22$	5	hH1/R1847K	$\tau_h^{fast} = 0.71 \pm 0.04$ $\tau_h^{slow} = 5.58 \pm 0.74$	3
hH1/E1810A	$\tau_h^{fast} = 0.55 \pm 0.03$ $\tau_h^{slow} = 5.20 \pm 0.11$	3	hH1/M1851L	$\tau_h^{fast} = 0.55 \pm 0.04$ $\tau_h^{slow} = 4.59 \pm 0.39$	6
hH1/V1813R	$\tau_h^{fast} = 0.51 \pm 0.02$ $\tau_h^{slow} = 4.98 \pm 0.10$	7	hH1/F1857L	$\tau_h^{fast} = 0.54 \pm 0.03$ $\tau_h^{slow} = 4.41 \pm 0.84$	6
hH1/A1818V	$\tau_h^{fast} = 0.61 \pm 0.11$ $\tau_h^{slow} = 4.08 \pm 0.23$	3	hH1/R1860E	$\tau_h^{fast} = 0.46 \pm 0.03$ $\tau_h^{slow} = 5.11 \pm 0.59$	7
hH1/A1820T	$\tau_h^{fast} = 0.73 \pm 0.06$ $\tau_h^{slow} = 5.71 \pm 0.34$	3	hH1/E1864D	$\tau_h^{fast} = 0.65 \pm 0.07$ $\tau_h^{slow} = 3.9 \pm 0.5$	4

n is the number of cells tested. None of the hH1 mutants had time constants of current decay that were statistically different from those of hH1.

A point mutation in this region causing long-QT syndrome has been recently identified (Deschênes et al., 2000). The mutation (E1784) was found to affect the inactivation of the channel resulting in a persistent sodium inward current. The residue is located beside one of the 20 amino acids that differs (T1783) between the two channels, and when it was replaced with its hSkM1 equivalent, a Serine residue, the phenotype of current decay kinetics was not modified. This result suggests that this residue is not responsible for the different behavior of the two isoforms. We concluded that most probably a combination of some of those 20 different amino acids would be responsible for differences in current-decay phenotypes between hH1 and hSkM1.

Interestingly, it is the C-terminal region that seems to confer the differences in the current-decay phenotype of the heart and skeletal muscle isoforms and not the inactivation gate that links the DIII and the DIV (West et al., 1992). The region formed by the S4-S5 linkers of domains III and IV (Filatov et al., 1998; McPhee et al., 1998; Smith & Goldin, 1997; Tang et al., 1996) would form the proposed receptor site of the inactivation particle. The present data also show that the differences in current decay are not species-dependent but rather tissue-specific. Thus, our results suggest for the first time a new structural region that is implicated in fast inactivation of voltage-gated sodium channels along with the inactivation gate. In a previous study, Sato and Matsumoto (1995) had also linked the C-terminal region to fast inactivation of sodium channels as suggested by their modeling studies. This role of the C-terminal region in current decay is also supported by the recent finding of mutations in the 100-amino-acid stretch of the C-terminus that cause long-QT syndrome (Wei et al., 1999; Deschênes et al., 2000). It is however, still unclear how and to what extent this region is involved in fast inactivation, but further structure-function studies will help us to understand its function.

This study was supported by the Heart and Stroke Foundation of Québec, the Canadian Institutes of Health Research MT-13181.

References

Armstrong, C.M., Bezanilla, F. 1977. Inactivation of the sodium channel. II. Gating current experiments. *J. Gen. Physiol.* **70:**567–590

Arreola, J., Spires, S., Begenisich, T. 1993. Na^+ channels in cardiac and neuronal cells derived from a mouse embryonal carcinoma cell line. *J. Physiol.* **472:**289–303

Auld, V.J., Goldin, A.L., Krafte, D.S., Catterall, W.A., Lester, H.A.,

Davidson, N., Dunn, R.J. 1990. A neutral amino acid change in segment IIS4 dramatically alters the gating properties of the voltage-dependent sodium channel. *Proc. Natl. Acad. Sci. USA* **87:**323–327

Backx, P.H., Yue, D.T., Lawrence, J.H., Marban, E., Tomaselli, G.F. 1992. Molecular localization of an ion-binding site within the pore of mammalian sodium channels. *Science* **257:**248–251

Bénitah, J.-P., Chen, Z., Balser, J.R., Tomaselli, G.F., Marbán, E. 1999. Molecular dynamics of the sodium channel pore vary with gating: interactions between P-segment motions and inactivation. *J. Neurosci.* **19:**1577–1585

Catterall, W.A. 1992. Cellular and molecular biology of voltage-gated sodium channels. *Physiol. Rev.* **72:**S15–S48

Cha, A., Ruben, P.C., George, Jr., A.L., Fujimoto, E., Bezanilla, F. 1999. Voltage sensors in domains III and IV, but not I and II, are immobilized by Na^+ channel fast inactivation. *Neuron* **22:**73–87

Chahine, M., Bennett, P.B., Horn, R., George, A.L. 1993. Functional expression of the human skeletal muscle sodium channel. *Biophys. J.* **64:**A4

Chahine, M., Deschênes, I., Chen, L.-Q., Kallen, R.G. 1996. Electrophysiological characteristics of cloned skeletal and cardiac muscle sodium channels expressed in tsA201 cells. *Am. J. Physiol.* **40:**H 498–H 506

Deschênes, I., Chen, L.-Q., Kallen, R.G., Chahine, M. 1998. Electrophysiological study of chimeric sodium channels from heart and skeletal muscle. *J. Membrane Biol.* **164:**25–34

Deschênes, I., Baroudi, G., Berthet, M., Barde, I., Chalvidan, T., Denjoy, I., Guicheney, P., Chahine, M. 2000. Electrophysiological characterization of *SCN5A* mutations causing long QT (E1784K) and Brugada (R1512W and R1432G) syndromes. *Cardiovasc. Res.* **46:**55–65

Eaholtz, G., Scheuer, T., Catterall, W.A. 1994. Restoration of inactivation and block of open sodium channels by an inactivation gate peptide. *Neuron* **12:**1041–1048

Filatov, G.N., Nguyen, T.P., Kraner, S.D., Barchi, R.L. 1998. Inactivation and secondary structure in the D/S4-5 region of the SkM1 sodium channel. *J. Gen. Physiol.* **111:**703–715

Frelin, C., Cognard, C., Vigne, P., Lazdunski, M. 1986. Tetrodotoxin-sensitive and tetrodotoxin-resistant Na^+ channels differ in their sensitivity to Cd^{2+} and Zn^{2+}. *Eur. J. Pharmacol.* **122:**245–250

Gellens, M.E., George, Jr., A.L., Chen, L., Chahine, M., Horn, R., Barchi, R.L., Kallen, R.G. 1992. Primary structure and functional expression of the human cardiac tetrodotoxin-insensitive voltage-dependent sodium channel. *Proc. Natl. Acad. Sci. USA* **89:**554–558

George, Jr., A.L., Komisarof, J., Kallen, R.G., Barchi, R.L. 1992. Primary structure of the adult human skeletal muscle voltage-dependent sodium channel. *Ann. Neurol.* **31:**131–137

Hamill, O.P., Marty, A., Neher, E., Sakmann, B., Sigworth, F.J. 1981. Improved patch-clamp techniques for high-resolution current recording from cells and cell-free membrane patches. *Pfluegers Arch.* **391:**85–100

Hodgkin, A.L., Huxley, A.F. 1952. A quantitative description of membrane current and its application to conduction and excitation in nerve. *J. Physiol.* **117:**500–544

Hoshi, T., Zagotta, W.N., Aldrich, R.W. 1990. Biophysical and molecular mechanisms of *shaker* potassium channel inactivation. *Science* **250:**533–538

Jurman, M.E., Boland, L.M., Liu, Y., Yellen, G. 1994. Visual identification of individual transfected cells for electrophysiology using antibody-coated beads. *Biotechniques* **17:**876–881

Kirsch, G.E., Brown, A.M. 1989. Kinetic properties of single sodium channels in rat heart and rat brain. *J. Gen. Physiol.* **93:**85–89

Ma, J.Y., Catterall, W.A., Scheuer, T. 1997. Persistent sodium currents through brain sodium channels induced by G protein $\beta\gamma$ subunits. *Neuron* **19:**443–452

Margolskee, R.F., McHendry-Rinde, B., Horn, R. 1993. Panning transfected cells for electrophysiological studies. *Biotechniques* **15:**906–911

McPhee, J.C., Ragsdale, D.S., Scheuer, T., Catterall, W.A. 1998. A critical role for the S4-S5 intracellular loop in domain IV of the sodium channel α-subunit in fast inactivation. *J. Biol. Chem.* **273:**1121–1129

Patton, D.E., West, J.W., Catterall, W.A., Goldin, A.L. 1992. Amino acid residues required for fast Na^+-channel inactivation: charge neutralizations and deletions in the III-IV linker. *Proc. Natl. Acad. Sci. USA* **89:**10905–10909

Pérez-García, M.T., Chiamvimonvat, N., Marban, E., Tomaselli, G.F. 1996. Structure of the sodium channel pore revealed by serial cysteine mutagenesis. *Proc. Natl. Acad. Sci. USA* **93:**300–304

Ravindran, A., Schild, L., Moczydlowski. E. 1991. Divalent cation selectivity for external block of voltage-dependent Na^+ channels prolonged by batrachotoxin. Zn^{2+} induces discrete substates in cardiac Na^+ channels. *J. Gen. Physiol.* **97:**89–115

Sato, C., Matsumoto, G. 1995. Sodium channel functioning based on an octagonal structure model. *J. Membrane Biol.* **147:**45–70

Schild, L., Moczydlowski, E. 1991. Competitive binding interaction between Zn^{2+} and saxitoxin in cardiac Na^+ channels. Evidence for a sulfhydryl group in the Zn^{2+}/saxitoxin binding site. *Biophys. J.* **59:**523–537

Smith, M.R., Goldin, A.L. 1997. Interaction between the sodium channel inactivation linker and domain III S4-S5. *Biophys. J.* **73:**1885–1895

Tang, L., Kallen, R.G., Horn, R. 1996. Role of an S4-S5 linker in sodium channel inactivation probed by mutagenesis and a peptide blocker. *J. Gen. Physiol.* **108:**89–104

Todt, H., Dudley, Jr., S.C., Kyle, J.W., French, R.J., Fozzard, H.A. 1999. Ultra-slow inactivation in μ1 Na^+ channels is produced by a structural rearrangement of the outer vestibule. *Biophys. J.* **76:** 1335–1345

Townsend, C., Horn, R. 1999. Interaction between the pore and a fast gate of the cardiac sodium channel. *J. Gen. Physiol.* **113:**321–331

Trimmer, J.S., Cooperman, S.S., Tomiko, S.A., Zhou, J., Crean, S.M., Boyle, M.B., Kallen, R.G., Sheng, Z., Barchi, R.L., Sigworth, F.J., Goodman, R.H., Agnew, W.S., Mandel, G. 1989. Primary structure and functional expression of a mammalian skeletal muscle sodium channel. *Neuron* **3:**33–49

Tsushima, R.G., Li, R.A., Backx, P.H. 1997. Altered ionic selectivity of the sodium-channel revealed by cysteine mutations within the pore. *J. Gen. Physiol.* **109:**463–475

Vassilev, P.M., Scheuer, T., Catterall, W.A. 1988. Identification of an intracellular peptide segment involved in sodium channel inactivation. *Science* **241:**1658–1661

Wang, D.W., George, Jr., A.L., Bennett, P.B. 1996. Comparison of heterologously expressed human cardiac and skeletal muscle sodium channels. *Biophys. J.* **70:**238–245

Wei, J., Wang, D.W., Alings, M., Fish, F., Wathen, M., Roden, D.M., George, Jr., A.L. 1999. Congenital long-QT syndrome caused by a novel mutation in a conserved acidic domain of the cardiac Na^+ channel. *Circulation* **99:**3165–3171

West, J.W., Patton, D.E., Scheuer, T., Wang, Y., Goldin, A.L., Catterall, W.A. 1992. A cluster of hydrophobic amino acid residues required for fast Na^+-channel inactivation. *Proc. Natl. Acad. Sci. USA* **89:**10910–10914

Yang, N.B., George, Jr., A.L., Horn, R. 1996. Molecular basis of charge movement in voltage-gated sodium channels. *Neuron* **16:**113–122

Yang, N.B., Horn, R. 1995. Evidence for voltage-dependent S4 movement in sodium channels. *Neuron* **15:**213–218